

Blind Extraction of Target Speech Source Guided by Supervised Speaker Identification via X-vectors

Jiri Malek, *Member, IEEE*, Jakub Jansky, Zbynek Koldovsky, *Senior member, IEEE*, Tomas Kounovsky, Jaroslav Cmejla and Jindrich Zdansky

Abstract—This manuscript proposes a novel robust procedure for extraction of a speaker of interest (SOI) from a mixture of audio sources. The estimation of the SOI is blind, performed via independent vector extraction. A recently proposed constant separating vector (CSV) model is employed, which improves the estimation of moving sources. The blind algorithm is guided towards the SOI via the frame-wise speaker identification, which is trained in a supervised manner and is independent of a specific scenario. When processing challenging data, an incorrect speaker may be extracted due to limitations of this guidance. To identify such cases, a criterion non-intrusively assessing quality of the estimated SOI is proposed. It utilizes the same model as the speaker identification; no additional training is therefore required. Using this criterion, the “deflation” approach to extraction is presented. If an incorrect source is estimated, it is subtracted from the mixture and the extraction of the SOI is performed again from the reduced mixture. The proposed procedure is experimentally tested on both artificial and real-world datasets containing challenging phenomena: source movements, reverberation, transient noise or microphone failures. The presented method is comparable to the state-of-the-art blind algorithms on static mixtures; it is more accurate for mixtures containing source movements. Compared to fully supervised methods, the proposed procedure achieves a lower level of accuracy but requires no scenario-specific data for the training.

Index Terms—Target speech extraction, blind extraction, supervised speaker identification.

I. INTRODUCTION

A frequent goal of speech processing is to recover a speaker of interest (SOI) from a mixture of speech sources and environmental noise. This task is often solved using *speech separation* methods; all sources present in the mixture are estimated and subsequently the SOI is identified among them. Separation can be performed in a supervised manner using principles of machine/deep learning [1]–[5] or without any prior information about the sources and the mixing using a blind approach [6]–[12].

The machine learning-based methods rely on scenario-specific information learned from the training/adaptation datasets [1]. They primarily perform spectral filtering using single-channel data, which can be supplemented by auxiliary spatial filtering, if additional channels are available. Due to both types of a utilized information, supervised methods often

provide higher separation quality compared to the blind approaches, when the test conditions strongly match the training ones. However, the supervised speech separation is often designed for fixed scenarios with a known number of active sources (or requires estimation thereof), which arguably limits its practicality/flexibility (see the discussion in [13]–[15]). The blind source separation (BSS) methods [6] do not require specific training data; the separation is based on statistical assumptions about the sources. In theory, blind methods can thus be applied to mixtures of an arbitrary number of sources active in an arbitrary environment. Many BSS methods perform spatial filtering, which requires multi-channel mixtures.

Focusing on blind methods, separation of speech usually proceeds in the time-frequency domain. Independent component analysis (ICA, [16]) separates the sources based on their statistical independence. For a wide-band signal, ICA is separately applied to each frequency bin, which leads to the so called *permutation ambiguity* [17]. The recovered frequency components have a random order and all components corresponding to the wide-band source need to be identified in order to reconstruct it in the time-domain. To alleviate this drawback, the independent vector analysis (IVA, [7], [8]) has been proposed. It binds together the frequency components corresponding to a single source using higher-order dependencies among them. Non-negative matrix factorization (NMF, [18]) attempts to factorize spectrogram of a single-channel mixture as a product of two non-negative components, recurring patterns and their activations. Multi-channel NMF (MNMF, [9]) extends this concept for analysis of multi-channel mixtures. Independent low-rank matrix analysis (ILRMA, [10]–[12]) unifies the principles of IVA and NMF. Spectral masking methods [19], [20] use the assumption that only one source is dominant at each time-frequency point.

For practical reasons, the separation is often limited exclusively to the SOI, which is referred to as target *speech extraction*. For deep-learning-based methods [13], [14], [21], [22], this approach eliminates the need for a known number of sources (or estimation thereof). In blind source extraction (BSE), it allows for relaxation of some constraints, e.g., the otherwise forbidden Gaussian distribution is allowed for the undesired/interfering sources [23].

The independent vector extraction (IVE) is a sub-problem of IVA focusing on the SOI [23]–[26]. The traditional model of IVE is time invariant, i.e., it is suitable for separation of immobile sources (*static approach*). To extract moving sources, the time invariant methods are consecutively applied to short intervals of data where the sources are approximately static,

This work was supported by the Technology Agency of the Czech Republic (Project No. TO01000027), by The Czech Science Foundation (Project No. 20-17720S) and by the Student Grant Scheme 2021 Project of the Technical University in Liberec.

All the authors were with the Faculty of Mechatronics, Informatics, and Interdisciplinary Studies, Technical University of Liberec, Studentská 2, 461 17, Liberec, Czech Republic. e-mail: (jiri.malek(at)tul.cz).

and their parameters are recursively updated. The drawback of this *block-wise static approach* [27] lies in difficult tuning of the block length and the recursion weight. Recently, an alternative approach based on the constant separating vector (CSV) model [28] has been proposed. It allows for changes of mixing parameters within the processed interval of data. Compared to the block-wise static approach, the CSV-based method exploits longer intervals of signals. Consequently, this allows us to achieve a higher extraction accuracy. This higher accuracy was proven theoretically in [29] and demonstrated experimentally in [30].

By definition, IVE methods extract an arbitrary source. To extract the SOI, an information identifying this source is required. Such information can be provided via a suitable initialization [31]; such initialization, however, does not guarantee that the method will remain focused on the SOI during updates. Alternatively, the extraction can be limited to a direction containing the SOI via the geometric constraint [32], [33], which requires a real-time localization for a moving SOI. A practical alternative is to introduce a *pilot signal* based on machine learning principles. This signal is related to the SOI and directs the convergence towards it. Piloting using voice activity detection was proposed for mixtures containing a single speaker in [34]. For mixtures of multiple speakers, pilots using supervised speaker identification [35], [36] via embeddings were proposed in [27].

Speaker embeddings are Deep-Neural-Network-based (DNN) features encoding the characteristics of a speaker. Several variants have recently been introduced, differing mainly in the topology of the extracting DNN. Embeddings derived from fully-connected feed-forward DNN were proposed in [37]. Approaches utilizing the context of the data via recursive long short-term memory (LSTM) networks were presented in [38]. The recursive modeling allows for more precise classification, however, the training is data-demanding and time-consuming.

To alleviate those demands, non-recursive topologies capturing the context have been proposed, such as time-delayed neural networks [39] (TDNN) or feed-forward sequential memory networks [40] (FSMN). The “context layers” within these networks process a set of frames (or feature vectors produced by their previous layer) centered around the current frame. The processing of the context significantly increases the number of learnable parameters. To reduce this number, TDNN sub-samples the set of frames, because the neighboring ones are assumed to be correlated. In contrast, FSMN weights all frames at an input of a layer by a trainable matrix and performs mean time-pooling. Thus FSMN can be seen as a generalization of TDNN in which the importance of frames is learned during training rather than selected during design.

This manuscript proposes a novel method for the extraction of SOI from realistic mixtures. The core of the method is an IVE algorithm endowed with the CSV mixing model. It focuses on the SOI using piloting based on the frame-wise speaker identification, similar to our previous works [27], [30]. An improvement for piloting is proposed by incorporation of a non-intrusive criterion for assessment of the extraction performance. The assessment allows for detection of the cases

in which an incorrect source is being extracted. These cases are treated by applying the deflation approach: the unwanted source is subtracted from the mixture, and the extraction is attempted again. This cycle continues until the SOI is estimated. The pilot signal as well as the criterion share the same pretrained FSMN model, which is fully independent of the extraction scenario. The proposed method is thus applicable to a wide variety of realistic mixtures without any additional adaptations. In comparison to our previous works, the properties and limitations of piloting are discussed in greater detail and experimentally demonstrated. The proposed extractor is verified using two widely analyzed datasets (CHiME-4 [41], the spatialized version of wsj0-2mix [2]) and an ad-hoc dataset featuring source movements. The benefits of deflation are demonstrated and the achieved results are compared to the state-of-the-art deep-learning-based and blind methods.

This article is organized as follows. The blind extraction algorithm is described in Section II-B. Section II-C provides the principles of piloting. The non-intrusive criterion for assessment of extraction quality is proposed in Section II-D. The deflation is presented in Section II-E. The proposed method is experimentally evaluated in Section III, while Section IV concludes the manuscript.

II. ALGORITHM DESCRIPTION

A. Problem definition

A time varying mixture of d original signals observed by d microphones can, in the short-time frequency domain, be approximated by the mixing model

$$\mathbf{x}_\ell^k = \mathbf{A}_\ell^k \mathbf{y}_\ell^k, \quad (1)$$

where $k = 1, \dots, K$ is the frequency and $\ell = 1, \dots, L$ is the frame index, \mathbf{y}_ℓ^k and \mathbf{x}_ℓ^k denote the original and mixed signals, respectively and \mathbf{A}_ℓ^k denotes the mixing matrix. For practical reasons, it is often assumed that the mixing is approximately static over a small number of subsequent frames. Let this interval be referred to as *block* in this manuscript. The mixture is thus divided into $t = 1, \dots, T$ equally long blocks of $\ell_t = 1, \dots, L_T$ frames, with a block-constant mixing matrix \mathbf{A}_t^k . The mixing model for this *block-wise static* approach [27] is given by

$$\mathbf{x}_{\ell_t}^k = \mathbf{A}_t^k \mathbf{y}_{\ell_t}^k \quad \text{for } t = 1, \dots, T. \quad (2)$$

Note that this model becomes fully static when $T = 1$ or maximally time-varying if $T = L$.

In IVA, a complete de-mixing matrix \mathbf{W}_t^k is sought such that it fulfills $\mathbf{W}_t^k \mathbf{x}_{\ell_t}^k = \mathbf{W}_t^k \mathbf{A}_t^k \mathbf{y}_{\ell_t}^k = \hat{\mathbf{y}}_{\ell_t}^k \approx \mathbf{y}_{\ell_t}^k$, i.e., it recovers all the sources present in the mixture. In contrast, IVE seeks only one row of \mathbf{W}_t^k , denoted by \mathbf{w}_t^k , such that it specifically extracts the SOI. Without any loss on generality, let the SOI be the first signal in $\mathbf{y}_{\ell_t}^k$ and \mathbf{A}_t^k be partitioned as $\mathbf{A}_t^k = [\mathbf{a}_t^k \quad \mathbf{Q}_t^k]$. Then, the equation (2) can be expressed in the form

$$\mathbf{x}_{\ell_t}^k = [\mathbf{a}_t^k \quad \mathbf{Q}_t^k] \begin{bmatrix} s_{\ell_t}^k \\ \mathbf{z}_{\ell_t}^k \end{bmatrix}, \quad (3)$$

where $s_{\ell_t}^k$ represents the SOI and $\mathbf{z}_{\ell_t}^k$ are the other $d - 1$ signals in the mixture. Subsequently, \mathbf{W}_t^k can be partitioned

as $[\mathbf{w}_t^k \ (\mathbf{B}_t^k)^H]^H$, where, \mathbf{B}_t^k is called a *blocking matrix* and \cdot^H denotes conjugate transpose.

B. Blind extraction: CSV-AuxIVE algorithm

The extraction part of the proposed procedure is a blind algorithm based on the CSV mixing model. The algorithm was derived in [28]; let us overview its most important ideas. The CSV model is based on an assumption that the separating vector \mathbf{w}_t^k is constant within all T blocks ($\mathbf{w}_t^k = \mathbf{w}^k, t = 1 \dots T$). This means that the separating vector obeys $(\mathbf{w}^k)^H \mathbf{x}_{\ell_t}^k = \hat{s}_{\ell_t}^k \approx s_{\ell_t}^k$ for each block t , where $\hat{s}_{\ell_t}^k$ is the SOI estimate. The mixing vector \mathbf{a}_t^k and the blocking matrix \mathbf{B}_t^k are still assumed to vary with respect to t .

The estimation of \mathbf{w}^k stems from the following *log-likelihood function*. Let $\mathbf{s}_{\ell_t} = [s_{\ell_t}^1 \dots s_{\ell_t}^K]$ be a vector of all frequency components corresponding to the SOI. The elements of \mathbf{s}_{ℓ_t} are assumed to be dependent; they thus need to be modeled by a joint pdf $p_s(\mathbf{s}_{\ell_t})$. The background signals $\mathbf{z}_{\ell_t}^1 \dots \mathbf{z}_{\ell_t}^K$ are Gaussian and their frequency components are assumed to be uncorrelated. Consequently, their higher order dependencies are zero and they can be modeled as independent; let their density be denoted $p_z(\mathbf{z}_{\ell_t}^k)$. The log-likelihood function is then

$$\mathcal{L}(\{\mathbf{w}^k\}_k, \{\mathbf{a}_t^k\}_k | \{\mathbf{x}_{\ell_t}^k\}_k) = \log p_s(\{\hat{s}_{\ell_t}^k\}_k) + \sum_{k=1}^K \log p_z(\hat{\mathbf{z}}_{\ell_t}^k) + \log |\det \mathbf{W}_t^k|^2, \quad (4)$$

where $\hat{\mathbf{z}}_{\ell_t}^k$ is the estimate of the background signals. The notation $\{\cdot\}_k$ describes a variable with all values of index k , e.g., $\{\mathbf{w}^k\}_k = \mathbf{w}^1, \dots, \mathbf{w}^K$.

Since the true $p_s(\mathbf{s}_{\ell_t})$ is unknown, an appropriate surrogate needs to be chosen. It has to take into account that the variance of the SOI potentially changes from block to block. The true values of the variances are unknown as well; they are therefore replaced by their sample-based estimates. Let $f(\cdot)$ be a pdf of a normalized non-Gaussian random variable, then $p_s(\mathbf{s}_{\ell_t})$ can be chosen as

$$p_s(\mathbf{s}_{\ell_t}) \approx f\left(\left\{\frac{s_{\ell_t}^k}{\hat{\sigma}_t^k}\right\}_k\right) \left(\prod_{k=1}^K \hat{\sigma}_t^k\right)^{-2}, \quad (5)$$

where $\hat{\sigma}_t^k = \sqrt{(\mathbf{w}^k)^H \hat{\mathbf{C}}_t^k \mathbf{w}^k}$ is the sample-based variance, $\hat{\mathbf{C}}_t^k = \hat{\mathbf{E}}_t[\mathbf{x}_{\ell_t}^k (\mathbf{x}_{\ell_t}^k)^H]$ is the sample-based covariance matrix of the mixture on the t th block and $\hat{\mathbf{E}}_t$ denotes the sample-based expectation over the frames in block t .

Using the assumption that all samples are independently distributed, the log-likelihood function (4) can be averaged over all blocks and samples. Following the derivations from [28], the *contrast function* is obtained in the form

$$\mathcal{C}(\{\mathbf{w}^k\}_k, \{\mathbf{a}_t^k\}_k) = \frac{1}{T} \sum_{t=1}^T \left\{ \mathbf{E}_t \left[\log f\left(\left\{\frac{(\mathbf{w}^k)^H \mathbf{x}_{\ell_t}^k}{\hat{\sigma}_t^k}\right\}_k\right) \right] - \sum_{k=1}^K \log(\hat{\sigma}_t^k)^2 - \sum_{k=1}^K \mathbf{E}_t[(\hat{\mathbf{z}}_{\ell_t}^k)^H (\mathbf{\Gamma}_t^k)^{-1} \hat{\mathbf{z}}_{\ell_t}^k] + \log |\det \mathbf{W}_t^k|^2 \right\}, \quad (6)$$

where \mathbf{E}_t denotes the expectation operator over the frames in block t and $\mathbf{\Gamma}_t^k$ is the covariance matrix of the background signals.

Optimization of (6) is performed using the *auxiliary function optimization* technique. The main idea is to replace the nonlinear contrast function with an auxiliary function $Q(\cdot)$, which is easier to optimize and retains the same optimal solution. Then the new auxiliary function is alternately optimized in original and auxiliary variables. Let the model density of the SOI be $f(x) \propto \exp\{-\|x\|\}$. Then the auxiliary function for (6) is obtained in the form

$$Q(\{\mathbf{w}^k, \mathbf{a}_t^k, \mathbf{V}_t^k\}_{k,t}) = \frac{1}{T} \sum_{t=1}^T \sum_{k=1}^K \left\{ -\frac{1}{2} \frac{(\mathbf{w}^k)^H \mathbf{V}_t^k \mathbf{w}^k}{(\hat{\sigma}_t^k)^2} - \log(\hat{\sigma}_t^k)^2 - \mathbf{E}_t[(\hat{\mathbf{z}}_{\ell_t}^k)^H (\mathbf{\Gamma}_t^k)^{-1} \hat{\mathbf{z}}_{\ell_t}^k] + \log |\det \mathbf{W}_t^k|^2 \right\} + R_t, \quad (7)$$

where

$$\mathbf{V}_t^k = \mathbf{E}_t[\varphi(r_{\ell_t}^k) \cdot \mathbf{x}_{\ell_t}^k (\mathbf{x}_{\ell_t}^k)^H], \quad (8)$$

$r_{\ell_t}^k$ are the auxiliary variables, R_t is a constant independent of \mathbf{w}^k and $\varphi(\cdot)$ is a suitable nonlinearity.

The final *update rules* are obtained by replacing the unknown expectation \mathbf{E}_t by its sample-based counterpart $\hat{\mathbf{E}}_t$ and by optimizing (7) alternately in the auxiliary ($r_{\ell_t}^k, \mathbf{V}_t^k$) and the original (\mathbf{w}^k) variables. The update rules are given by:

$$r_{\ell_t}^k = \sqrt{\sum_{k=1}^K |(\mathbf{w}^k)^H \mathbf{x}_{\ell_t}^k|^2} \quad \text{for all } \ell_t, \quad (9)$$

$$\mathbf{V}_t^k = \hat{\mathbf{E}}_t[\varphi(r_{\ell_t}^k) \mathbf{x}_{\ell_t}^k (\mathbf{x}_{\ell_t}^k)^H], \quad (10)$$

$$\hat{\mathbf{C}}_t^k = \hat{\mathbf{E}}_t[\mathbf{x}_{\ell_t}^k (\mathbf{x}_{\ell_t}^k)^H], \quad (11)$$

$$\mathbf{a}_t^k = \frac{\hat{\mathbf{C}}_t^k \mathbf{w}^k}{(\mathbf{w}^k)^H \hat{\mathbf{C}}_t^k \mathbf{w}^k}, \quad (12)$$

$$\hat{\sigma}_{k,t} = \sqrt{(\mathbf{w}^k)^H \hat{\mathbf{C}}_t^k \mathbf{w}^k}, \quad (13)$$

$$\mathbf{w}^k = \left(\sum_{t=1}^T \frac{\mathbf{V}_t^k}{(\hat{\sigma}_t^k)^2} \right)^{-1} \sum_{t=1}^T \frac{(\mathbf{w}^k)^H \mathbf{V}_t^k \mathbf{w}^k}{(\hat{\sigma}_t^k)^2} \mathbf{a}_t^k, \quad (14)$$

where (12) is the *orthogonal constraint* (OGC) ensuring mutual orthogonality of \mathbf{w}^k and \mathbf{a}_t^k . A normalization $\mathbf{w}^k \leftarrow \mathbf{w}^k / \sqrt{\sum_{t=1}^T (\mathbf{w}^k)^H \mathbf{V}_t^k \mathbf{w}^k}$ is performed after each iteration to enable stable convergence. Note that for $T = 1$ the algorithm coincides with the auxiliary function-based static IVE approach from [24].

C. Extraction guided towards the SOI: piloting

Without any prior information concerning the SOI, CSV-AuxIVE extracts an arbitrary source from the mixture. We introduce the prior information in the form of a pilot signal [42] related to the SOI, which directs the convergence towards the SOI. The pilot \mathbf{g} is independent of the mixing model parameters and thus does not change the analytic learning rules

of CSV-AuxIVE. The only difference is that the non-linearity $\varphi(\cdot)$ now depends on \mathbf{g} , i.e., the update step in (9) changes to

$$r_{\ell_t}^k = \sqrt{\sum_{k=1}^K |(\mathbf{w}^k)^H \mathbf{x}_{\ell_t}^k|^2 + g_{\ell_t}}. \quad (15)$$

This change stems from the fact that the right-hand side of (9) corresponds to a factor that binds together all frequency components belonging to a single source. Through addition of \mathbf{g} , the frequency components become also dependent on the SOI. The rest of the CSV-AuxIVE algorithm remains unchanged.

A suitable candidate for \mathbf{g} is the mixture in those intervals in which the energy of the other sources is low (the SOI is *dominant*). We propose to compute the pilot signal \mathbf{g} for the ℓ th frame (note that \mathbf{g} is independent of CSV blocks) as

$$g_{\ell} = \begin{cases} \sum_{k=1}^K |x_{\ell}^k(1)|^2 & \text{the SOI is dominant,} \\ 0 & \text{otherwise,} \end{cases} \quad (16)$$

where $x_{\ell}^k(1)$ is the mixture on the first microphone.

Two variants of a pilot signal are considered in this manuscript. 1) The realizable \mathbf{g}^{XVEC} , which is based on principles of the speaker identification via pre-trained embeddings. It is defined in Section II-C3. 2) An *ideal oracle pilot* \mathbf{g}^{ORAC} , which is used to analyze the possibilities of piloting. It cannot be used in practice, because it requires the unobservable energies of the sources. \mathbf{g}^{ORAC} is computed using (16), where SOI is considered dominant within the ℓ th frame if

$$\sum_{k=1}^K |s_{\ell}^k|^2 > \mu_{\text{ORAC}} \sum_{k=1}^K \|\mathbf{z}_{\ell}^k\|^2 \text{ and } \sum_{k=1}^K |s_{\ell}^k|^2 > \mu_{\text{ENE}}(s), \quad (17)$$

where μ_{ORAC} is a free parameter reflecting the desired level of dominance and $\mu_{\text{ENE}}(s)$ is a minimum energy, where the SOI is still considered active.

1) *Network topology for embedding extraction, X-vectors:* Our implementation of the embedding network stems from the FSMN¹ architecture [40] and is summarized in Table I. Its input consists of a single-channel audio signal sampled at 16 kHz. The input features are 40 filter bank coefficients computed from frames of a length of 400 and a frame-shift of 200 samples. Subsequently, six Context layers are present, i.e., context of frames is weighted by a trainable matrix; mean time-pooling is performed; and a linear transformation is applied. The output of each layer is weighted by the exponential linear unit (ELU). The Pooling layer computes variances of frames. Its context length is $L_c = 101$ during training. The network is trained to classify N speakers via minimization of the cross-entropy loss function.

After training, the two latest classification layers are removed and the embeddings are extracted from the Pooling layer. This is done to allow for classification of the speakers absent in the training set. In the test phase, an embedding of an unknown speaker is compared to the set of embeddings (called *enrollment*) corresponding to the potential speakers. This

¹The utilized network topology does not differ from our previous works in [27], [30]. There we described the embedding network as TDNN with modifications. A more detailed research of literature revealed that it is more accurate to label the network as FSMN.

TABLE I: Description of the FSMN producing the X-vectors. The input sizes for the context layers are stated after the mean pooling operation.

Layer	Layer context	Total context	Input x output
Context 1	$\ell \pm 80$	161	40×1024
Context 2	$\ell \pm 4$	169	1024×768
Context 3	$\ell \pm 4$	177	768×512
Context 4	$\ell \pm 4$	185	512×384
Context 5	$\ell \pm 4$	193	384×256
Context 6	$\ell \pm 4$	201	256×128
Fully-conn. 1	ℓ	201	128×128
Pooling	$\ell \pm \frac{L_c - 1}{2}$	$201 + L_c$	$(L_c \cdot 128) \times 128$
Fully-conn. 2	ℓ	$201 + L_c$	128×128
Softmax	—	$201 + L_c$	$128 \times N$

comparison is performed by Probabilistic Linear Discriminant Analysis (PLDA, [43]). PLDA is a machine learning approach that tests a hypothesis that a pair of embedding vectors corresponds to a single speaker. The statistical distributions necessary for this testing are derived from a training dataset of precomputed embeddings. PLDA returns a score, which is high if the hypothesis is correct.

In this manuscript, we denote the extracted embeddings as *X-vectors*. In the narrow sense, this term is reserved for features estimated by the TDNN [35]. However, since both topologies are closely related, we believe such naming can be used without ambiguity.

2) *Training datasets and their augmentation:* The training data for the FSMN and PLDA originate from the development part of the Voxceleb database [44] and the training part of the LibriSpeech corpus [45]. The Voxceleb utterances contain real-world reverberation and noise. Librispeech (part train-360-clean) is free of distortions. It was subjected to augmentations discussed below, in order to train X-vectors robust with respect to environmental distortions. The environmental noise was taken from the simulated part of the CHiME-4 training dataset [41] and the development dataset available in Task 1 of the DCASE2018 challenge [46].

The augmented X-vectors were trained on one unchanged instance of Voxceleb/Librispeech and three augmented instances of the Librispeech dataset, where the following augmentations were applied:

- 1) Reverberation: The utterances were convolved with artificial room impulse responses (RIRs) generated by [47]. The artificial RIRs originated from a shoe-box room of size $8 \times 7 \times 3$ m; four different reverberation times T_{60} , ranging from 175–650 ms, were considered. The source-microphone distance was 1–2 m.
- 2) Noise: The environmental noise was summed with the original Librispeech utterances at signal-to-noise-ratio (SNR) equal to 10 dB.
- 3) Reverberation+noise: The noise was added to the reverberated Librispeech dataset with SNR= 10 dB.

The PLDA was trained using the three augmented variants of the Librispeech dataset.

3) *Frame-wise speaker identification for piloting:* Conventionally, speaker identification operates on long intervals/sentences. Piloting requires information localized to a

short interval centered around the current frame. To obtain such a sequence of X-vectors, the input context of the TDNN is gradually shifted by a single frame. For each shift, an X-vector is computed based on pooling with a shortened context (e.g., $L_c = 11$). Moreover, speaker identification for piloting differs from the conventional one in the following aspects.

- The identification is performed in the presence of cross-talk. However, only *the dominant speaker* is of interest.
- Only the *identity/dominance of the SOI is important*; it must not be confused with any interfering speaker. However, substitution within the set of interferers is irrelevant because the pilot in (16) is set to zero regardless of the identity of the interfering source.
- The size of the enrollment set is significantly smaller. Conventionally, hundreds of speakers need to be distinguished. For the purposes of piloting, only several potential speakers (e.g., eighteen) are considered.

The short context of the Pooling layer and the aspect a) complicate the identification task, whereas the aspects b) and c) simplify it.

To perform frame-wise identification, PLDA scores $M_\ell(\xi, \chi_{x_\ell})$ are computed. Here, ξ is the enrollment X-vector corresponding to one of the potential speakers and χ_{x_ℓ} is the X-vector computed using the context around the ℓ th frame within the first channel of the mixture. The speaker with the highest $M_\ell(\xi, \chi_{x_\ell})$ is the most distinctive from the perspective of the X-vectors and is also *assumed to be dominant* in the mixture. Validity of this assumption is experimentally verified in Section III-D1.

Using the scores $M_\ell(\xi, \chi_{x_\ell})$, the *X-vector-based pilot* \mathbf{g}^{XVEC} is computed according to (16), where the SOI is considered dominant in the ℓ th frame if

$$\begin{aligned} M_\ell(\xi_s, \chi_{x_\ell}) &> \max\{M_\ell(\xi_{z_j}, \chi_{x_\ell}), j = 1 \dots J\} \quad \text{and} \\ M_\ell(\xi_s, \chi_{x_\ell}) &> \mu_{\text{PLDA}}(\xi_s), \end{aligned} \quad (18)$$

where ξ_s denotes the X-vector corresponding to the SOI and $\mu_{\text{PLDA}}(\xi_s)$ is the lowest PLDA score, where the SOI is still considered active. The variable ξ_{z_j} denotes the X-vector corresponding to the j th potential interfering speaker from the enrollment set containing the SOI and J other speakers. The properties and limitations of piloting are demonstrated experimentally in Section III-D.

D. Non-intrusive assessment of extraction quality

This Section proposes a non-intrusive criterion to assess whether the extraction of the SOI was successful. This criterion is based on the same X-vectors and PLDA as the piloting, i.e., no additional training is required.

The assessment represents the entire signal through a single PLDA score $M(\xi_s, \cdot)$ independent of ℓ (FSMN pooling context is set $L_c = L$). As in conventional speaker identification, this score can be seen as a measure of similarity between the X-vector computed from the enrollment utterance of the SOI and an unknown test X-vector. When the SOI is active²

²SOI is considered active in the test utterance when its PLDA score $M(\xi_s, \cdot)$ is one of the highest compared to the other enrollment speakers.

Algorithm 1 Deflation mechanism for CSV-AuxIVE using the extraction assessment. Variables χ_s^i and χ_x^i denote X-vectors corresponding to the SOI estimate and the first channel of the mixture after i deflation steps.

Require: Multi-channel mixture \mathbf{x}_ℓ^k , X-vector FSMN, enrollment set including the SOI, PLDA model

```

for  $i \leftarrow 0, i < I$  do
  Extract  $\hat{\mathbf{s}}_{\ell_t}^{k,i}$  from  $\mathbf{x}_{\ell_t}^{k,i}$  using piloted CSV-AuxIVE
  if  $M(\xi_s, \chi_s^i) > M(\xi_s, \chi_x^i)$  then
    return  $\hat{\mathbf{s}}_{\ell_t}^{k,i}$  {Extracted source is the SOI estimate}
  else
     $\mathbf{x}_{\ell_t}^{k,i+1} \leftarrow$  Subtract  $\hat{\mathbf{s}}_{\ell_t}^{k,i}$  from  $\mathbf{x}_{\ell_t}^{k,i}$  using (19)
    if  $M(\xi_s, \chi_x^i) > M(\xi_s, \chi_x^{i+1})$  then
      return  $\mathbf{x}_{\ell_t}^{k,i}$  {Reduced mixture is not closer to the SOI, end the deflation}
    else
      {Continue the deflation}
    end if
  end if
end for
return  $\mathbf{x}_{\ell_t}^{k,i+1}$  {Maximum number of steps reached}

```

in the test utterance, its score $M(\xi_s, \cdot)$ is high; the presence of distortions decreases the similarity/score. Based on these observations, the *extraction assessment* is proposed:

Assessment (of extraction quality). *Having X-vectors for two variants of the same signal³ with an active SOI denoted by χ_{s_1}, χ_{s_2} ; if $M(\xi_s, \chi_{s_1}) > M(\xi_s, \chi_{s_2})$ then χ_{s_1} corresponds to a superior estimate of the SOI in the sense of speech quality.*

The extraction assessment is experimentally validated in Section III-E. The Section shows a strong linear dependence between increments in criteria measuring quality of speech and the PLDA score. The extraction assessment is used in the deflation process as a *decision mechanism*. It determines whether the extracted source is an estimate of the SOI or of an unwanted source (and deflation should be applied).

E. Re-estimation of the SOI on extraction failure: deflation

The deflation provides a mechanism to extract the SOI from mixtures in which the desired source is difficult to identify via pilot alone. This may happen, e.g., when the SOI is the weaker source and only a small number of frames with dominant SOI exist to form an efficient pilot.

The deflation is summarized in Algorithm 1 and proceeds as follows. The first signal is extracted using the piloted CSV-AuxIVE. The extraction assessment is used to determine whether this signal represents a better estimate of the SOI than the original mixture. If so, the first signal is returned and the extraction ends. Otherwise, the first signal is subtracted from the mixture (on each CSV block) using least square projection. Using the assessment, the reduced mixture is compared to the original one. If the original mixture is chosen, the extraction ends (the deflation did not bring the mixture closer to the SOI).

³For example, the original mixture and the extracted signal.

If the reduced mixture is selected, the piloted CSV-AuxIVE is applied to it and the second signal is extracted. This process is repeated until an estimate of the SOI is found or until a predefined number I of deflation steps has been performed.

Let $\mathbf{x}_{\ell_t}^{k,i}$ and $\mathbf{w}^{k,i}$ denote the input mixture and the separating vector after i deflation steps, respectively. The reduced mixture $\mathbf{x}_{\ell_t}^{k,i+1}$ is obtained by the least square subtraction of the extracted signal $\hat{\mathbf{s}}_{\ell_t}^{k,i} = (\mathbf{w}^{k,i})^H \mathbf{x}_{\ell_t}^{k,i}$ from $\mathbf{x}_{\ell_t}^{k,i}$. Let $\mathbf{a}_t^{k,i}$ be the mixing vector after i deflation steps computed on the t th block via (12). Due to the orthogonality of $\mathbf{w}^{k,i}$ and $\mathbf{a}_t^{k,i}$, the subtraction is achieved through

$$\mathbf{x}_{\ell_t}^{k,i+1} = \mathbf{D}^{k,i} (\mathbf{x}_{\ell_t}^{k,i} - \mathbf{a}_t^{k,i} (\mathbf{w}^{k,i})^H \mathbf{x}_{\ell_t}^{k,i}), \quad (19)$$

where $\mathbf{D}^{k,i}$ is a $(d-i-1) \times (d-i)$ full row-rank matrix, reducing the dimension of $\mathbf{x}_{\ell_t}^{k,i+1}$ by one compared to $\mathbf{x}_{\ell_t}^{k,i}$. This reduction needs to be applied to avoid rank deficiency of the “deflated” mixture. Matrix $\mathbf{D}^{k,i}$ can be found via principal component analysis [48] or can simply omit one element of $\mathbf{x}_{\ell_t}^{k,i}$.

III. EXPERIMENTS

The following experiments pursue three goals. 1) The possibilities and limitations of piloting are investigated as a motivation for the proposed deflation. 2) The functionality of the proposed extraction assessment is analyzed. 3) The benefits of the deflation are demonstrated and the performance of the proposed extractor is compared to results published in the literature.

A. Datasets

The experiments are performed on the following three datasets, which contain various detrimental phenomena such as source movements, high reverberation and noise activity, transients or low energy of the SOI.

1) *Dynamic dataset*: The first dataset is an ad-hoc simulated one containing noisy recordings of two simultaneously active moving speakers (SOI and interfering source (IS)). The sources are located in a room of dimensions $6 \times 6 \times 3$ m; reverberation times $T_{60} \in \{100, 300, 600\}$ ms are considered. A linear array of five omni-directional microphones with spacings of 8 cm is placed close to the center of the room and rotated counter-clockwise by 45° . Both sources move on a half-circle around the array, the radius is 1.5 m for the SOI and 2 m for the IS. SOI performs a large angular movement in the left-hand half-plane and IS a small one in the right-hand half-plane. A static directional noise source is located perpendicular to the microphone array axis to the right. The situation is depicted in Figure 1.

The speech (sampled at 16 kHz) originates from the test/development sets of CHiME-4; four potential speakers (F01, F06, M04, M05) are considered. The cafeteria noise used for directional noise originates from the QUT corpus [49]. Different utterances are concatenated to form 5 unique test signals of length 25 s for each speaker. The movements of SOI and positions of the static sources are simulated using the RIR generator [47]. One instance of the experiment (for one T_{60} value) thus consists of 300 mixtures (6 speaker combinations

$\times 2$ speaker roles $\times 25$ utterance combinations). The sources are mixed at an input signal-to-interference-ratio of 0 dB (SIR, ratio of energy of SOI and IS) and an input signal-to-noise-ratio of 10 dB (SNR, ratio of all speech to noise energy).

2) *CHiME-4 dataset*: CHiME-4 dataset [41] contains six-channel real-world and simulated recordings of a single speaker active in a highly noisy environment. The dataset does not contain cross-talk; however, the real-world part contains a lot of microphone failures and transient noises. These non-speech signals are occasionally extracted instead of SOI.

3) *Multi-channel Wall Street Journal - 2mix dataset*: The multi-channel version of the Wall Street Journal - 2mix dataset (MC-WSJ0-2mix, [2]) is currently often used to compare speaker separation and extraction algorithms. The MC-WSJ0-2mix dataset contains 3,000 simulated mixtures recorded in a reverberant environment using a microphone array containing eight microphones. Each mixture contains two active speakers, i.e., there is 6,000 extraction experiments in total. The sources are mixed with SIR between $\langle -5, +5 \rangle$ dB. Some of the recordings are very short; their durations range from 1.6 s to 13.9 s. The recordings are highly reverberant ($T_{60} \in \langle 200, 600 \rangle$ ms), and captured in rooms with variable dimensions. The topology of the microphone array is varying, as well as the source-microphone distance, which is 1.3 m with 0.4 m standard deviation. The dataset does not contain environmental noise or source movements. The 8 kHz variant of the mixtures is used.

B. Evaluation measures and common settings

The extraction is evaluated in terms of the following metrics. SIR and SDR are computed using BSS_EVAL [50]. The perceptual quality of the extracted sources is quantified using the “perceptual evaluation of speech quality” (PESQ [51]) or “short-time objective intelligibility measure” (STOI, [52]). These metrics are evaluated over the entire signal lengths with the exception of the Dynamic dataset, for which (due to source movements) the measures are evaluated within intervals of length 1 s each and subsequently averaged.

When the extraction algorithm fails to track a moving SOI (the SOI moves out of the spatial focus of the method), the desired speech vanishes from the estimated signal. To measure this phenomenon, we also provide *the standard deviation* of the “SOI Attenuation” metric, defined as $\sum_k |\hat{s}_\ell^k|^2 / \sum_k |s_\ell^k|^2$, where \hat{s}_ℓ^k is the estimate of s_ℓ^k . For a properly extracted moving SOI, this deviation should be close to zero and it increases if the gain of the desired speech fluctuates.

All the experiments have been performed without any adaptation of the algorithm or the FSMN network to a specific scenario. The enrollment set always consists of 1 minute of speech for each target speaker considered in the given scenario, augmented by reverberation as described in Section II-C. The FSMN pooling context length is $L_c = 11$.

C. CSV model for extraction of a moving SOI

This experiment is performed on the Dynamic dataset. It demonstrates the benefits of the CSV-model on mixtures with moving sources and the ability of \mathbf{g}^{XVEC} to direct the

TABLE II: Dynamic dataset: the extraction performance of the CSV-AuxIVE (CSV $_{L_T}$), the static (FS-IVE) and the block-wise static (BS-IVE $_{L_T}$) IVE techniques. The subscript L_T denotes the number of frames within the analyzed block.

Method	Pilot	iPESQ			SDR [dB]			iSIR [dB]			Attenuation		
		100ms	300ms	600ms	100ms	300ms	600ms	100ms	300ms	600ms	100ms	300ms	600ms
FS-IVE	-	0.32	0.05	-0.01	7.96	0.19	-2.58	15.33	6.97	4.04	0.42	0.17	0.10
FS-IVE	\mathbf{g}^{ORAC}	0.61	0.22	0.11	9.17	3.88	0.98	19.72	13.31	9.72	0.32	0.19	0.12
FS-IVE	\mathbf{g}^{XVEC}	0.51	0.14	0.04	8.40	2.45	-1.21	18.46	11.16	6.61	0.33	0.18	0.10
CSV $_{200}$	-	0.49	0.11	0.02	9.01	1.35	-1.72	17.03	7.60	4.60	0.36	0.15	0.10
CSV $_{200}$	\mathbf{g}^{ORAC}	0.87	0.27	0.13	12.64	4.72	1.29	22.01	13.29	9.64	0.25	0.13	0.10
CSV $_{200}$	\mathbf{g}^{XVEC}	0.76	0.20	0.06	11.36	3.37	-0.61	20.46	11.38	6.85	0.28	0.14	0.10
BS-IVE $_{200}$	-	0.09	-0.00	-0.07	4.11	0.07	-2.19	12.50	6.53	4.17	0.32	0.18	0.14
BS-IVE $_{200}$	\mathbf{g}^{ORAC}	0.39	0.16	0.05	9.23	4.68	1.60	19.34	13.54	9.92	0.26	0.17	0.14
BS-IVE $_{200}$	\mathbf{g}^{XVEC}	0.22	0.04	-0.05	6.45	1.75	-1.31	15.69	9.25	5.69	0.28	0.17	0.13
CSV $_{800}$	\mathbf{g}^{XVEC}	0.52	0.15	0.03	8.17	2.25	-1.38	18.11	10.68	6.17	0.32	0.17	0.10
BS-IVE $_{800}$	\mathbf{g}^{XVEC}	0.42	0.11	0.00	7.79	2.38	-1.06	18.11	10.35	5.91	0.31	0.19	0.13
CSV $_{50}$	\mathbf{g}^{XVEC}	0.60	0.14	0.02	11.59	2.94	-0.67	17.63	8.47	4.45	0.16	0.11	0.10
BS-IVE $_{50}$	\mathbf{g}^{XVEC}	0.04	-0.03	-0.10	3.89	0.67	-1.86	11.83	7.63	4.85	0.23	0.15	0.12

extraction towards the SOI. The results of CSV-AuxIVE are compared to the fully static (FS-IVE, [24]) and the block-wise static (BS-IVE, [30]) variants of AuxIVE.

CSV-AuxIVE and FS-IVE process the entire mixture as a single segment using 50 iterations. BS-IVE applies 5 iterations to each block of length L_T and shift $L_T/4$ frames. The inner statistics in BS-IVE are accumulated using recursive forgetting with $\alpha = 0.3$ (see [27]). All these methods are initialized using the location of the SOI at the beginning of the recording; BS-IVE initializes the extraction at each block by the solution from the previous one. The NFFT length is 1,024 and shift 200 samples. The threshold $\mu_{\text{ORAC}} = 2$.

All criteria in Table II indicate that the pilot-guided methods extract the SOI more precisely than the methods relying on initialization (without any pilot). Due to the limited identification accuracy, the performance with \mathbf{g}^{XVEC} is inferior to that with \mathbf{g}^{ORAC} (by 1.6 – 2.8 dB of iSIR). The CSV-AuxIVE achieves superior (or at least comparable) performance compared to its static or block-wise static counterparts. This is notable especially when \mathbf{g}^{XVEC} is used. CSV-AuxIVE appears to be more robust than BS-IVE with respect to pilot inaccuracies.

The important parameter of CSV-AuxIVE/BS-IVE is the length of block L_T , which influences the compromise between adaptivity to movement and the amount of available data. Excessively long blocks (FS-IVE or BS-IVE $_{800}$) yield high iSIR and PESQ but also increase Attenuation compared to the suitable block length (BS-IVE $_{200}$). Using long blocks, the methods are unable to adapt well to the source movements and the SOI moves out of their spatial focus (the sound vanishes for certain time intervals).⁴ The increased Attenuation is observable for the CSV $_{800}$ as well; the increase of iSIR/PESQ is, however, not present. The prolongation of inner blocks does not bring the advantage of more available data. Application of an insufficiently short block (50 frames) allows for good adaptation (low SOI Attenuation), but the overall IS suppression is deteriorating (low iSIR).

⁴Note that the Attenuation describes the vanishing of the SOI well for $T_{60} \leq 300$ ms but fails to capture this phenomenon for more reverberant scenario. We can observe that this fact is due to the reverberation of the SOI, which is still present in the estimate even when the location (direct path) of the SOI lies outside of the spatial focus of the methods.

D. Properties and limitations of piloting

This Section analyzes the accuracy of the frame-wise speaker identification and its influence on the extraction. Subsequently, the causes of pilot failures are discussed.

1) *The frame-wise dominant speaker identification:* As a reference in this task, we use the identity of the speaker with the highest energy in the mixture. This energy is computed using the same context of frames as the pooling context of FSMN ($L_c \in \{7, 11, 21\}$, i.e., $\{9, 14, 26\}$ ms). The most reverberant part ($T_{60} = 600$ ms) of the Dynamic dataset is revisited. Multiple variants of this dataset are considered, each changing the input SIR $\in \{-5, 0, 5, 10, 20\}$ dB and the input SNR $\in \{0, 10, \infty\}$ dB. Markers in Figs. 2 and 3 correspond to the averaged accuracy over all mixtures in one such variant.

Let us first verify the assumption that the source with the highest PLDA score is also the dominant one in the mixture. Considering $L_c = 11$ and the noiseless case, Fig. 2 confirms our assumption with the accuracy ranging from 59% – 77%. By definition of the pilot in (16), the identity of the interfering speaker is irrelevant for \mathbf{g}^{XVEC} . The classification is thus simplified to a binary task whether the SOI or an arbitrary other source is dominant. Fig. 3 shows that the accuracy of SOI dominance identification is 69% – 77%. The presence of noise decreases the accuracy to 63% – 73%. The results of the extraction in the previous Section indicate that such accuracy leads to a functional \mathbf{g}^{XVEC} , which improves the performance of CSV-AuxIVE by iSIR= 2.3 dB over its non-piloted counterpart. Utilization of \mathbf{g}^{ORAC} leads to another increase by 2.8 dB.

It might seem surprising that accuracy of SOI dominance identification is high despite the low SIR. This is caused by a low occurrence of frames with a dominant SOI (for SIR= -5 dB, only 28.5% of frames). The classifier is thus often correct when it assigns the frame to the easily classifiable interfering source with high energy.

A short context of the pooling layer L_c is required for the frame-wise identification. However, it deteriorates the accuracy due to the increased variability of the X-vectors (less data is available for the pooling). Figs. 2 and 3 indicate that this accuracy is, as expected, highest for $L_c = 21$ and monotonically deteriorates with decreasing L_c . On the other

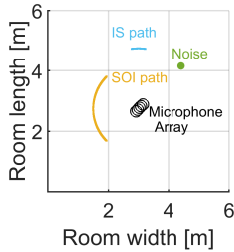


Fig. 1: Source trajectories and locations for the Dynamic dataset.

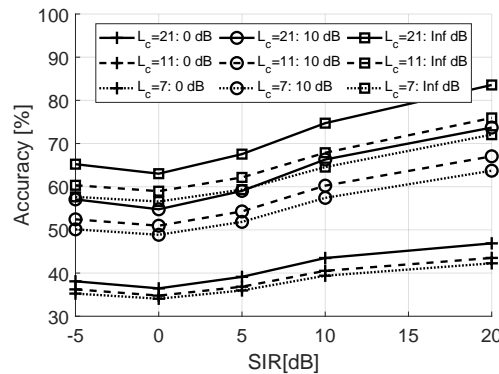


Fig. 2: Accuracy in the task of the dominant speaker identification; each marker corresponds to a different SNR.

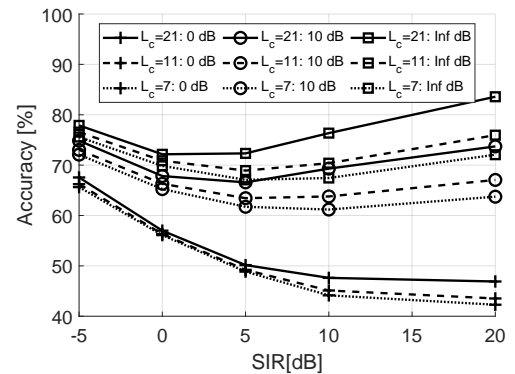


Fig. 3: Accuracy in the task of the SOI dominance identification; each marker corresponds to a different SNR.

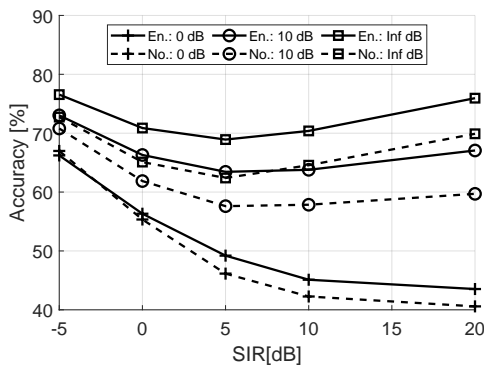


Fig. 4: Accuracy in the task of the SOI dominance identification with respect to language of speakers in the enrollment set; $L_c = 11$ and each marker corresponds to a different SNR.

TABLE III: Dynamic dataset: the extraction performance of piloted CSV-AuxIVE ($L_T = 200$) with respect to X-vector context L_c .

Context L_c	SDR [dB]			iSIR [dB]		
	100ms	300ms	600ms	100ms	300ms	600ms
7	11.37	3.38	-0.67	20.48	11.40	6.71
11	11.36	3.37	-0.61	20.46	11.38	6.85
21	11.19	3.18	-0.68	20.14	10.87	6.64

hand, Table III shows that the long context $L_c = 21$ achieves the worst extraction performance; the piloting is no longer well localized in time. As a compromise, context $L_c = 11$ is utilized throughout this manuscript.

2) *Language dependence of the SOI identification*: The blind CSV-AuxIVE algorithm is language independent. However, piloting using g^{XVEC} is based on deep-learning and thus is designed to work on English language present in the training dataset. Its accuracy might deteriorate if applied to an unseen language. To quantify, this scenario compares the SOI identification/extraction achieved on English with results yielded on unseen Norwegian. It analyzes a slightly modified version of the Dynamic dataset. The original English speakers are replaced by four Norwegian (2 male and 2 female) originating in the NST speech database [53].

TABLE IV: Dynamic dataset: the extraction performance with respect to spoken language (English or Norwegian); the language dependence of g^{XVEC} . The subscript L_T denotes the number of frames within the analyzed block.

Method	Pilot	Lang.	iPESQ		SDR [dB]		iSIR [dB]	
			100ms	600ms	100ms	600ms	100ms	600ms
CSV ₂₀₀	-	Eng.	0.49	0.02	9.01	-1.72	17.03	4.60
CSV ₂₀₀	g^{ORAC}	Eng.	0.87	0.13	12.64	1.29	22.01	9.64
CSV ₂₀₀	g^{XVEC}	Eng.	0.76	0.06	11.36	-0.61	20.46	6.85
CSV ₂₀₀	-	Nor.	0.42	-0.01	7.74	-2.65	15.05	2.62
CSV ₂₀₀	g^{ORAC}	Nor.	0.81	0.11	12.92	1.27	22.42	9.70
CSV ₂₀₀	g^{XVEC}	Nor.	0.74	0.02	11.51	-1.06	20.86	6.02

The results in Figure 4 corroborate that X-vectors are slightly language dependent; the accuracy for Norwegian speakers is lower by about 4.5%. However, this does not influence the extraction performance much. The metrics in Table IV indicate that the non-piloted extraction is slightly less accurate for the Norwegian dataset. This decrease does not stem from the language as such but it is caused by longer silences between Norwegian sentences. When the SOI is quiet, the non-piloted extractor tends to converge to an arbitrary active source. The utilization of a pilot completely removes this difference. The results for CSV-AuxIVE piloted via g^{XVEC} are comparable for both datasets (difference is lower than 1 dB iSIR and 0.5 dB SDR); the proposed method can thus be considered language independent in this experiment.

3) *Limitations of the embedding-based piloting in low SIR scenarios*: By definition in (16), the pilot is non-zero/active when the SOI is dominant in a subset of frames. This condition becomes difficult to fulfill when SIR is low. Let us demonstrate using mixtures in the Dynamic dataset. Considering three levels of $SIR = \{20, 0, -5\}$ dB; the SOI is dominant in 93.2%, 48.3% and 28.5% of frames, respectively. For a low SIR, the potential support is limited, which weakens the guidance provided by the pilot. g^{XVEC} suffers from a further reduction of the support, because it incorrectly identifies a subset of the dominant frames. An extreme case of the pilot being equal to zero for all frames leads to non-piloted extraction (which, moreover, tends to extract the dominant interfering source).

TABLE V: MC-WSJ0-2mix: the number of failed extraction cases (SDR < -2 dB) for piloted CSV-AuxIVE using 4 channels.

Pilot/deflation	Failed cases
No pilot	2986
g^{XVEC}	680
g^{XVEC} + deflation	58
g^{ORAC}	24

The deflation approach provides a mechanism to alleviate these limitations. Let us demonstrate via an extraction experiment on MC-WSJ0-2mix dataset [2]. The dataset contains 3,000 mixtures of two active speakers. Since each of the speakers can assume the role of the SOI, 6,000 independent extractions can be performed. Let us observe the number of the failed extraction cases with respect to the type of the piloting in Table V. The non-piloted CSV-AuxIVE fails in 2,986 cases. It has no way to focus on a specific SOI and, in addition, fails to process several mixtures (output SDR is close to 0 dB). g^{XVEC} reduces the fail rate by about 77 % to 680 cases; in 440 of these mixtures, the SOI is the weaker source (input SDR < 0 dB). The deflation significantly reduces the number to 58 cases, which is comparable to the utilization of g^{ORAC} .

E. Non-intrusive assessment of extraction quality

In this Section, we verify whether the PLDA score can be used to select a superior SOI estimate within several available variants. The superiority is measured using the standard objective and perceptual metrics (SIR, SDR, STOI).

In this experiment, we use the simulated development part of CHiME-4, which contains 1,640 sentences produced by 4 speakers. The CSV-AuxIVE with uniform initialization is applied to these recordings and stopped consecutively after {0, 5, 10, 15, 20, 25} iterations. For each utterance and each stop, the PLDA score $M(\xi_s, \chi_{\hat{s}})$ and the metrics are evaluated. Subsequently, the differences with respect to the previous stop are computed, because the goal is to find the relationship between the change of $M(\xi_s, \chi_{\hat{s}})$ and the change in metrics.

The differences plotted in Fig. 5 indicate the existence of a linear dependence. The Pearson correlation coefficient reaches a value of 0.82 for STOI. From another perspective, the assessment can also be perceived as a binary classifier: given the increase/decrease of $M(\xi_s, \chi_{\hat{s}})$, we want to predict the respective change in the objective criterion. Table VI shows that the classification accuracy is 72.7 % and 69.2 % for SIR and STOI, respectively. There are two types of error: 1) False positives ($M(\xi_s, \chi_{\hat{s}})$ increases, but the metrics decrease) are more serious and potentially lead us to selecting an interfering source. Fortunately, there is a negligible number of cases with significant deterioration, a decrease worse than 1dB in SIR happens only in 0.3% cases. 2) False negatives ($M(\xi_s, \chi_{\hat{s}})$ decreases, but criteria increase) potentially lead us to selecting of an inferior estimate. There is a 7.9% proportion of the cases exhibiting a significant decrease in SIR, but a rather low number of significant decreases in SDR and STOI (2.7% and 0.8% respectively). This indicates that the extraction

TABLE VI: CHiME-4 (simulated development part): the evaluation of the proposed extraction assessment from the perspective of a binary classifier. Significant cases denote samples in which the erroneous increase/decrease in SIR/SDR is larger than 1dB or 0.01 in STOI.

	SIR	SDR	STOI
Correlation coefficient [-]	0.64	0.74	0.82
Accuracy[%]	72.7	70.4	69.2
False positives [%]	5.7	15.3	20.2
Significant false positives [%]	0.3	1.2	1.6
False negatives [%]	21.6	14.2	10.5
Significant false negatives [%]	7.9	2.7	0.8

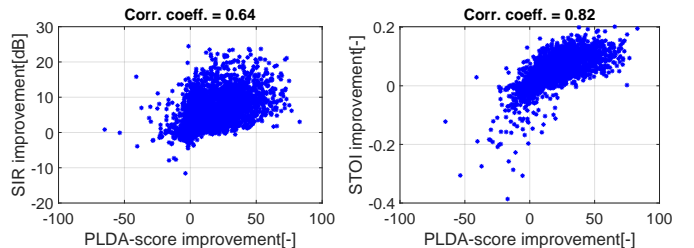


Fig. 5: CHiME-4 (simulated development part): dependency between the improvements of the objective criteria and the improvements of PLDA score.

assessment prefers solutions that are less distorted at the cost of lower noise attenuation.

F. Extraction via deflation on public datasets

The following experiments provide comparison between results achieved by the proposed method and the results reported in the literature. The experiments also show benefits brought by deflation.

1) *Extraction of the SOI from noisy recordings with transients and microphone failures:* Piloting and deflation should not be necessary on CHiME-4 data since the recordings contain only one active speaker. However, the real-world part of CHiME-4 is sometimes distorted by transients and microphone failures. These signals behave like sources that are strongly non-Gaussian, which have wide areas of attraction in contrast functions of blind algorithms. Therefore, they are often extracted instead of speech. The piloting and deflation used in our method provide effective solutions for this phenomenon.

The enhancement via piloted CSV-AuxIVE is compared with two enhancers known to be very successful on the CHiME-4 data: BeamformIt [54], a weighted delay-and-sum beamformer, which is used as a front-end algorithm in the original CHiME-4 baseline system. The Generalized Eigenvalue Beamformer (GEV) is a front-end solution proposed in [55], [56]. The latter represents one of the most successful enhancers for CHiME-4. It relies on voice activity detection (VAD) via deep networks trained specifically for the CHiME-4 data. We utilize the feed-forward topology of the VAD (the training procedure was kindly provided to us by the authors of [55]) and re-train the network using the training part of the CHiME-4 data.

TABLE VII: WER [%] yielded on the real-world part of the CHiME-4 datasets. Mixture results are achieved using data from channel 5.

	Mix. ch.5.	Beamform-It	GEV	CSV	CSV +pilot	CSV +pilot +defl.
Dev.	9.8	5.8	4.6	5.8	5.4	5.4
Test	19.9	11.5	8.1	9.9	9.5	9.3

Since the true references of the sources are not available for the real-world part of CHiME-4, the experiments are evaluated using the WER of the original baseline recognizer from [57]. All of the proposed methods are initialized by the relative transfer function estimator from [58]. CSV-AuxIVE performs 5 iterations in the STFT domain with an FFT length of 512, hop-size of 200 (the shift of the FSMN network) and applied Hamming window; the sampling frequency is 16 kHz. The length of the CSV-AuxIVE block is 2 seconds ($L_T = 160$ frames). The enrollment set for piloting contains 8 speakers; respective speech signals originate from the simulated development part of CHiME-4.

The results in Table VII indicate that the WER of CSV-AuxIVE⁵ is lowered by using piloting and further using deflation. This is in agreement with the discussion presented in Section III-D3: namely, the piloting significantly reduces the number of diverged cases and the deflation allows for re-estimation of the SOI when the piloting fails. The proposed method yields lower WER values compared to BeamformIt but is still outperformed by GEV. Nevertheless, GEV is a technique specifically tailored to CHiME-4 due to dataset-specific VAD and is limited to enhancement of recordings without cross-talk. In contrast, the proposed technique is, without adaptation, applicable to both speech enhancement and extraction. Even without piloting, CSV-AuxIVE achieves results approaching those of GEV without a need for training.

2) *Extraction of the SOI from cross-talk in a reverberant environment*: The following experiment compares the performance of the proposed method on the MC-WSJ0-2mix dataset to the results reported in the literature. The competing methods can be divided into three groups: 1) Oracle methods representing ideal extractors. These methods cannot be used in practice as they utilize information that is normally not available. 2) Methods based on machine learning (ML), which rely on the existence of a scenario-specific training dataset. 3) Blind source separation/extraction methods, which exploit spatial information extracted from the multi-channel mixture.

For ML-based methods, we consider approaches that perform both the SOI identification and estimation. For blind approaches, the literature usually presents methods performing a complete separation (BSS). Here, all sources in the mixture are estimated and the SOI is subsequently identified among them in an oracle manner (for the evaluation). In contrast, the piloted CSV-AuxIVE only extracts (BSE) the SOI.

The oracle approaches are represented by the 1) multi-channel Wiener filter (MCWF), which uses the oracle covari-

⁵Slightly different WER of CSV-AuxIVE was reported in [28]; it is caused by a different FFT frame-shift and the number of performed iterations.

TABLE VIII: MC-WSJ0-2mix: SDR [dB] yielded using machine-learning (ML), blind source separation (BSS with oracle speaker identification) and blind source extraction (BSE). The column “Tr. data” quantifies the volume of the required scenario-specific training data.

Approach	Chan. num.	Tr. data [hrs.]	Separation	Spk. id.	SDR [dB]
Mixture	-	-	-	-	0.2
MCWF	2	-	Orac.	Orac.	9.0
MCWF	4	-	Orac.	Orac.	13.4
TasNet [3]	2	50	ML	ML	8.4
FD-SpkBeam [13]	2	50	ML	ML	7.9
TD-SpkBeam-Orig. [13]	2	50	ML	ML	11.5
TD-SpkBeam-Ext. [22]	2	50	ML	ML	12.9
ILRMA [11]	2	-	BSS	Orac.	5.9
GCC-NMF [18]	2	-	BSS	Orac.	2.7
MESSL [19]	2	-	BSS	Orac.	3.3
CSV ₁₆₀ + g ^{ORAC}	2	-	BSE	Orac.	5.4
FS-IVE + g ^{XVEC} + defl.	2	-	BSE	ML	4.5
CSV ₁₆₀ + g ^{XVEC} + defl.	2	-	BSE	ML	4.1
ILRMA [11]	4	-	BSS	Orac.	7.6
GLOSS [20]	4	-	BSS	Orac.	9.3
CSV ₁₆₀ + g ^{ORAC}	4	-	BSE	Orac.	9.6
FS-IVE + g ^{XVEC} + defl.	4	-	BSE	ML	7.7
CSV ₁₆₀ + g ^{XVEC} + defl.	4	-	BSE	ML	7.8
CSV ₁₆₀ + g ^{XVEC}	4	-	BSE	ML	6.0

ance matrix of the target speech and constitutes the upper boundary for the extraction based on spatial filtering. The machine learning-based separation is represented by: 2) TasNet from [3], which is based on a convolutional topology performing full separation in the time domain; subsequently, the SOI is selected via speaker identification. 3) The frequency (FD) and time domain (TD) variants of SpeakerBeam [13], [22], which perform speaker extraction based on an enrollment utterance. Blind methods are represented by 4) masking-based binaural MESSL [19], 5) binaural GCC-NMF [18] based on non-negative matrix factorization, 6) consistent ILRMA from [11], 7) GLOSS [20] using sparsity-based spectral masking and single-channel post-filter and 8) static auxiliary function-based independent vector extraction FS-IVE [24].

These methods are evaluated in terms of SDR implemented in the BSS_EVAL toolbox [50]. CSV-AuxIVE operates in the STFT domain with an FFT length of 1,000, a hop-size of 100 (the shift of the FSMN network), and an applied Hamming window; the sampling frequency is 8 kHz. The length of the CSV-AuxIVE block is 2 seconds. The enrollment set contains 18 speakers; the X-vectors are computed using unused sentences from the original WSJ0 dataset. For the extraction, only the identity of the SOI (not the IS) is known. The publicly available implementation⁶ of consistent ILRMA [11] is used. ILRMA (using 100 iterations) and MCWF⁷ were applied in the STFT domain with window length of 1024 and hop-size 512 samples. The results for TasNet were taken over from [13]; for MESSL and GCC-NMF, they were found in [2]. The other results originate from their respective references.

⁶<https://github.com/d-kitamura/ILRMA>

⁷Different results of MCWF reported in [2] are caused by a short STFT length of 256 used there.

Restricting the methods to two channels, the results presented in Table VIII show that the ML-based spatial+spectral filtering outperforms the blind spatial filtering by a large margin. The supervised methods are even comparable to oracle MCWF using two/four microphones. This is possible due to the existence of a strictly matching training part of the MC-WSJ0-2mix dataset. In this setting, CSV-AuxIVE with \mathbf{g}^{XVEC} and deflation outperforms MESSL and GCC-NMF. Using \mathbf{g}^{ORAC} , CSV-AuxIVE yields SDR comparable to ILRMA.

The two-channel setting is, however, arguably unfair for blind methods relying solely on spatial diversity of the sources. Utilization of four channels increases the SDR for all blind methods. Using \mathbf{g}^{XVEC} , deflation and 4 microphones, CSV-AuxIVE is comparable to ML-based FD-SpeakerBeam and blind ILRMA performing full separation. Using \mathbf{g}^{ORAC} , CSV-AuxIVE achieves results comparable to GLOSS. The results confirm that CSV-AuxIVE coincides with FS-IVE if the mixed sources are static. The best performance overall is achieved by the variants of TD-SpeakerBeam, which approach the oracle MCWF using 4 channels.

Concerning the benefits of deflation, the failures of \mathbf{g}^{XVEC} (discussed in Section III-D3), caused by a weak SOI activity and limited classification accuracy, deteriorate significantly the average SDR. Considering 4 microphones, CSV-AuxIVE using \mathbf{g}^{XVEC} yields SDR lower by 3.6 dB compared to CSV-AuxIVE using \mathbf{g}^{ORAC} . The deflation partly alleviates this issue and increases the average SDR by 1.8 dB.

IV. CONCLUSIONS

This manuscript presents a blind target speech extraction approach (CSV-AuxIVE), guided towards the desired source by the supervised speaker identification. The estimation of the SOI is ensured through two techniques: the piloting and the successive deflation of the multi-source mixture. Evaluation of the proposed approach leads to the following conclusions: 1) The presented frame-wise SOI identification applied to mixtures exhibits accuracy of 67% in highly reverberated and noisy scenarios ($T_{60} = 600$ ms and $\text{SIR} = 0$ dB). 2) This accuracy is sufficient to form an efficient pilot to direct the extraction in most scenarios. However, the embedding-based piloting fails when the mixture contains a small number of frames where the SOI is dominant, such as when the activity of the SOI is short and has a low energy level. These cases can be remedied using successive deflation of the mixture along with the re-estimation of the SOI. 3) The proposed non-intrusive assessment of extraction quality can successfully be used as a decision mechanism to determine whether the deflation should be applied. It is strongly correlated with the objective/perceptual criteria used to evaluate quality of speech; the Pearson coefficient between PLDA score and STOI improvements reaches a value of 0.82. 4) The procedure as a whole is language independent. The accuracy of the speaker identification deteriorates slightly for an unseen language, but this has negligible effect on the extraction. 5) The CSV-AuxIVE achieves more precise extraction compared to the blind block-wise static approach for mixtures of moving sources. On mixtures of static sources,

the piloted CSV-AuxIVE is comparably accurate to competing blind approaches performing full separation followed by the oracle source identification. 6) The proposed approach achieves a lower performance compared to the state-of-the-art machine learning-based algorithms, as observed on widely known CHiME-4 and MC-WSJ0-2mix datasets. On the other hand, it does not require any scenario-specific training data or adaptation procedures.

REFERENCES

- [1] D. Wang and J. Chen, "Supervised speech separation based on deep learning: An overview," *IEEE/ACM Transactions on Audio, Speech, and Language Processing*, vol. 26, no. 10, pp. 1702–1726, 2018.
- [2] Z.-Q. Wang, J. Le Roux, and J. R. Hershey, "Multi-channel deep clustering: Discriminative spectral and spatial embeddings for speaker-independent speech separation," in *2018 IEEE International Conference on Acoustics, Speech and Signal Processing (ICASSP)*. IEEE, 2018, pp. 1–5.
- [3] Y. Luo and N. Mesgarani, "Conv-tasnet: Surpassing ideal time-frequency magnitude masking for speech separation," *IEEE/ACM transactions on audio, speech, and language processing*, vol. 27, no. 8, pp. 1256–1266, 2019.
- [4] M. Togami, "End to end learning for convolutive multi-channel wiener filtering," in *2021 IEEE International Conference on Acoustics, Speech and Signal Processing (ICASSP)*. IEEE, 2021, pp. 8032–8036.
- [5] C. Boeddeker, W. Zhang, T. Nakatani, K. Kinoshita, T. Ochiai, M. Delcroix, N. Kamo, Y. Qian, and R. Haeb-Umbach, "Convolutive transfer function invariant sdr training criteria for multi-channel reverberant speech separation," in *2021 IEEE International Conference on Acoustics, Speech and Signal Processing (ICASSP)*. IEEE, 2021, pp. 8428–8432.
- [6] E. Vincent, T. Virtanen, and S. Gannot, *Audio Source Separation and Speech Enhancement*. Wiley Publishing, 2018.
- [7] T. Kim, H. T. Attias, S.-Y. Lee, and T.-W. Lee, "Blind source separation exploiting higher-order frequency dependencies," *IEEE transactions on audio, speech, and language processing*, vol. 15, no. 1, pp. 70–79, 2006.
- [8] R. Scheibler and M. Togami, "Surrogate source model learning for determined source separation," in *2021 IEEE International Conference on Acoustics, Speech and Signal Processing (ICASSP)*. IEEE, 2021, pp. 176–180.
- [9] K. Sekiguchi, Y. Bando, A. A. Nugraha, M. Fontaine, and K. Yoshii, "Autoregressive fast multichannel nonnegative matrix factorization for joint blind source separation and dereverberation," in *2021 IEEE International Conference on Acoustics, Speech and Signal Processing (ICASSP)*. IEEE, 2021, pp. 511–515.
- [10] D. Kitamura, N. Ono, H. Sawada, H. Kameoka, and H. Saruwatari, "Determined blind source separation unifying independent vector analysis and nonnegative matrix factorization," *IEEE/ACM Transactions on Audio, Speech, and Language Processing*, vol. 24, no. 9, pp. 1626–1641, 2016.
- [11] D. Kitamura and K. Yatabe, "Consistent independent low-rank matrix analysis for determined blind source separation," *EURASIP Journal on Advances in Signal Processing*, vol. 2020, no. 1, pp. 1–35, 2020.
- [12] T. Nakashima, R. Scheibler, M. Togami, and N. Ono, "Joint dereverberation and separation with iterative source steering," in *2021 IEEE International Conference on Acoustics, Speech and Signal Processing (ICASSP)*. IEEE, 2021, pp. 216–220.
- [13] M. Delcroix, T. Ochiai, K. Zmolikova, K. Kinoshita, N. Tawara, T. Nakatani, and S. Araki, "Improving speaker discrimination of target speech extraction with time-domain speakerbeam," in *2020 IEEE International Conference on Acoustics, Speech and Signal Processing (ICASSP)*. IEEE, 2020, pp. 691–695.
- [14] M. Ge, C. Xu, L. Wang, E. S. Chng, J. Dang, and H. Li, "Multi-stage speaker extraction with utterance and frame-level reference signals," in *2021 IEEE International Conference on Acoustics, Speech and Signal Processing (ICASSP)*. IEEE, 2021, pp. 6109–6113.
- [15] M. Delcroix, K. Zmolikova, T. Ochiai, K. Kinoshita, and T. Nakatani, "Speaker activity driven neural speech extraction," in *2021 IEEE International Conference on Acoustics, Speech and Signal Processing (ICASSP)*. IEEE, 2021, pp. 6099–6103.
- [16] A. Hyvärinen, J. Karhunen, and E. Oja, *Independent Component Analysis*. John Wiley & Sons, 2001.

- [17] H. Sawada, R. Mukai, S. Araki, and S. Makino, "A robust and precise method for solving the permutation problem of frequency-domain blind source separation," in *IEEE transactions on speech and audio processing*, Apr. 2003, pp. 505–510.
- [18] S. U. Wood, J. Rouat, S. Dupont, and G. Pironkov, "Blind speech separation and enhancement with GCC-NMF," *IEEE/ACM Transactions on Audio, Speech, and Language Processing*, vol. 25, no. 4, pp. 745–755, 2017.
- [19] M. I. Mandel, R. J. Weiss, and D. P. W. Ellis, "Model-based expectation maximization source separation and localization," *IEEE Trans. Audio, Speech and Language Processing*, vol. 18, pp. 382–394, Feb. 2010.
- [20] B. Laufer-Goldshtein, R. Talmon, and S. Gannot, "Global and local simplex representations for multichannel source separation," *IEEE/ACM Transactions on Audio, Speech, and Language Processing*, vol. 28, pp. 914–928, 2020.
- [21] K. Žmolíková, M. Delcroix, K. Kinoshita, T. Ochiai, T. Nakatani, L. Burget, and J. Černocký, "Speakerbeam: Speaker aware neural network for target speaker extraction in speech mixtures," *IEEE Journal of Selected Topics in Signal Processing*, vol. 13, no. 4, pp. 800–814, 2019.
- [22] J. Han, X. Zhou, Y. Long, and Y. Li, "Multi-channel target speech extraction with channel decorrelation and target speaker adaptation," in *2021 IEEE International Conference on Acoustics, Speech and Signal Processing (ICASSP)*. IEEE, 2021, pp. 6094–6098.
- [23] Z. Koldovsky and P. Tichavsky, "Gradient algorithms for complex non-gaussian independent component/vector extraction, question of convergence," *IEEE Transactions on Signal Processing*, vol. 67, no. 4, pp. 1050–1064, Feb 2019.
- [24] R. Scheibler and N. Ono, "Independent vector analysis with more microphones than sources," in *2019 IEEE Workshop on Applications of Signal Processing to Audio and Acoustics (WASPAA)*. IEEE, 2019, pp. 185–189.
- [25] R. Ikeshita, T. Nakatani, and S. Araki, "Overdetermined independent vector analysis," in *2020 IEEE International Conference on Acoustics, Speech and Signal Processing (ICASSP)*. IEEE, 2020, pp. 591–595.
- [26] R. Ikeshita and T. Nakatani, "Independent vector extraction for fast joint blind source separation and dereverberation," *IEEE Signal Processing Letters*, 2021.
- [27] J. Jansky, J. Malek, J. Cmejla, T. Kounovsky, Z. Koldovsky, and J. Zdansky, "Adaptive blind audio source extraction supervised by dominant speaker identification using X-vectors," in *2020 IEEE International Conference on Acoustics, Speech and Signal Processing (ICASSP)*. IEEE, 2020, pp. 676–680.
- [28] J. Jansky, Z. Koldovsky, J. Malek, T. Kounovsky, and J. Cmejla, "Auxiliary function-based algorithm for blind extraction of a moving speaker," *arXiv preprint arXiv:2002.12619v2*, 2021.
- [29] V. Kautský, Z. Koldovský, P. Tichavský, and V. Zarzoso, "Cramér-rao bounds for complex-valued independent component extraction: Determined and piecewise determined mixing models," *IEEE Transactions on Signal Processing*, vol. 68, pp. 5230–5243, 2020.
- [30] J. Malek, J. Jansky, T. Kounovsky, Z. Koldovsky, and J. Zdansky, "Blind extraction of moving audio source in a challenging environment supported by speaker identification via x-vectors," in *2021 IEEE International Conference on Acoustics, Speech and Signal Processing (ICASSP)*. IEEE, 2021, pp. 226–230.
- [31] Y. Liang, S. M. Naqvi, and J. A. Chambers, "Audio video based fast fixed-point independent vector analysis for multisource separation in a room environment," *EURASIP Journal on Advances in Signal Processing*, vol. 2012, no. 1, p. 183, 2012.
- [32] A. Brendel, T. Haubner, and W. Kellermann, "A unified probabilistic view on spatially informed source separation and extraction based on independent vector analysis," *IEEE Transactions on Signal Processing*, vol. 68, pp. 3545–3558, 2020.
- [33] —, "Spatially guided independent vector analysis," in *2020 IEEE International Conference on Acoustics, Speech and Signal Processing (ICASSP)*. IEEE, 2020, pp. 596–600.
- [34] F. Nesta, S. Mosayyebpour, Z. Koldovsky, and K. Palecek, "Audio/video supervised independent vector analysis through multimodal pilot dependent components," in *2017 25th European Signal Processing Conference (EUSIPCO)*. IEEE, 2017, pp. 1150–1164.
- [35] D. Snyder, D. Garcia-Romero, G. Sell, D. Povey, and S. Khudanpur, "X-vectors: Robust DNN embeddings for speaker recognition," in *2018 IEEE International Conference on Acoustics, Speech and Signal Processing (ICASSP)*. IEEE, 2018, pp. 5329–5333.
- [36] D. Garcia-Romero, D. Snyder, G. Sell, D. Povey, and A. McCree, "Speaker diarization using deep neural network embeddings," in *2017 IEEE International Conference on Acoustics, Speech and Signal Processing (ICASSP)*. IEEE, 2017, pp. 4930–4934.
- [37] E. Variani, X. Lei, E. McDermott, I. L. Moreno, and J. Gonzalez-Dominguez, "Deep neural networks for small footprint text-dependent speaker verification," in *2014 IEEE International Conference on Acoustics, Speech and Signal Processing (ICASSP)*. IEEE, 2014, pp. 4052–4056.
- [38] G. Heigold, I. Moreno, S. Bengio, and N. Shazeer, "End-to-end text-dependent speaker verification," in *2016 IEEE International Conference on Acoustics, Speech and Signal Processing (ICASSP)*. IEEE, 2016, pp. 5115–5119.
- [39] V. Peddinti, D. Povey, and S. Khudanpur, "A time delay neural network architecture for efficient modeling of long temporal contexts," in *Sixteenth Annual Conference of the International Speech Communication Association*, 2015.
- [40] S. Zhang, C. Liu, H. Jiang, S. Wei, L. Dai, and Y. Hu, "Feedforward sequential memory networks: A new structure to learn long-term dependency," *arXiv preprint arXiv:1512.08301*, 2015.
- [41] E. Vincent, S. Watanabe, A. A. Nugraha, J. Barker, and R. Marxer, "The 4th CHiME speech separation and recognition challenge [online]," accessed: 29.9.2021. [Online]. Available: http://spandh.dcs.shef.ac.uk/chime_challenge/chime2016/
- [42] F. Nesta and Z. Koldovsky, "Supervised independent vector analysis through pilot dependent components," in *2017 IEEE International Conference on Acoustics, Speech and Signal Processing (ICASSP)*. IEEE, 2017, pp. 536–540.
- [43] S. Ioffe, "Probabilistic linear discriminant analysis," in *European Conference on Computer Vision*. Springer, 2006, pp. 531–542.
- [44] A. Nagrani, J. S. Chung, and A. Zisserman, "Voxceleb: a large-scale speaker identification dataset," *arXiv preprint arXiv:1706.08612*, 2017.
- [45] V. Panayotov, G. Chen, D. Povey, and S. Khudanpur, "Librispeech: an ASR corpus based on public domain audio books," in *2015 IEEE International Conference on Acoustics, Speech and Signal Processing (ICASSP)*. IEEE, 2015, pp. 5206–5210.
- [46] "DCASE 2018 challenge [online]," accessed: 29.9.2021. [Online]. Available: <http://dcase.community/challenge2018/index>
- [47] E. A. Habets, "Room impulse response generator," *Technische Universiteit Eindhoven, Tech. Rep.*, vol. 2, no. 2.4, p. 1, 2006.
- [48] I. Jolliffe, "Principal component analysis," *Encyclopedia of statistics in behavioral science*, 2005.
- [49] D. B. Dean, S. Sridharan, R. J. Vogt, and M. W. Mason, "The QUT-NOISE-TIMIT corpus for the evaluation of voice activity detection algorithms," *Proceedings of Interspeech 2010*, 2010.
- [50] E. Vincent, R. Gribonval, and C. Fevotte, "Performance measurement in blind audio source separation," *IEEE transactions on audio, speech, and language processing*, vol. 14, no. 4, pp. 1462–1469, July 2006.
- [51] A. W. Rix, J. G. Beerends, M. P. Hollier, and A. P. Hekstra, "Perceptual evaluation of speech quality (PESQ)—a new method for speech quality assessment of telephone networks and codecs," in *2001 IEEE International Conference on Acoustics, Speech and Signal Processing (ICASSP)*, vol. 2. IEEE, 2001, pp. 749–752.
- [52] C. H. Taal, R. C. Hendriks, R. Heusdens, and J. Jensen, "An algorithm for intelligibility prediction of time–frequency weighted noisy speech," *IEEE Transactions on Audio, Speech, and Language Processing*, vol. 19, no. 7, pp. 2125–2136, 2011.
- [53] G. Andersen, "NST norwegian asr database [online]," accessed: 29.9.2021. [Online]. Available: <https://www.nb.no/sprakbanken/en/resource-catalogue/oai-nb-no-sbr-13/>
- [54] X. Anguera, C. Wooters, and J. Hernando, "Acoustic beamforming for speaker diarization of meetings," *IEEE Transactions on Audio, Speech, and Language Processing*, vol. 15, no. 7, pp. 2011–2022, 2007.
- [55] J. Heymann, L. Drude, and R. Haeb-Umbach, "Neural network based spectral mask estimation for acoustic beamforming," in *2016 IEEE International Conference on Acoustics, Speech and Signal Processing (ICASSP)*, March 2016, pp. 196–200.
- [56] —, "Wide residual BLSTM network with discriminative speaker adaptation for robust speech recognition," in *Proc. of the 4th Intl. Workshop on Speech Processing in Everyday Environments, CHiME-4*, 2016.
- [57] E. Vincent, S. Watanabe, A. A. Nugraha, J. Barker, and R. Marxer, "An analysis of environment, microphone and data simulation mismatches in robust speech recognition," *Computer Speech & Language*, 2016.
- [58] S. Gannot, D. Burshtein, and E. Weinstein, "Signal enhancement using beamforming and nonstationarity with applications to speech," *IEEE Transactions on Signal Processing*, vol. 49, no. 8, pp. 1614–1626, Aug 2001.